Vibrational Spectroscopy

International Edition: DOI: 10.1002/anie.201600350
German Edition: DOI: 10.1002/ange.201600350

Characterization of the Oxygen Binding Motif in a Ruthenium Water Oxidation Catalyst by Vibrational Spectroscopy

*Erin M. Duffy, Brett M. Marsh, Jonathan M. Voss, and Etienne Garand**

Abstract: *For homogeneous mononuclear ruthenium water oxidation catalysts, the Ru–O_2 complex plays a crucial role in the rate determining step of the catalytic cycle, but the exact nature of this complex is unclear. Herein, the infrared spectra of the $[Ru(tpy)(bpy)(O_2)]^{2+}$ complex (tpy = 2,2′:6′,2″-terpyridine; bpy = 2,2′-bipyridine) are presented. The complex $[Ru(tpy)(bpy)(O_2)]^{2+}$, formed by gas-phase reaction of $[Ru(tpy)(bpy)]^{2+}$ with molecular O_2, was isolated by using mass spectrometry and was directly probed by cryogenic ion IR predissociation spectroscopy. Well-resolved spectral features enable a clear identification of the O–O stretch using $^{18}O_2$ substitution. The band frequency and intensity indicate that the O_2 moiety binds to the Ru center in a side-on, bidentate manner. Comparisons with DFT calculations highlight the shortcomings of the B3LYP functional in properly depicting the Ru–O_2 interaction.*

Catalytic mediation of water oxidation continues to be a topic of significant interest even after decades of research.[1–3] In more recent years, mononuclear ruthenium complexes with polypyridyl ligands have grown rapidly in importance as water oxidation catalysts (WOCs).[4–8] Detailed kinetic studies[9,10] of a family of $[Ru(tpy)(L)(H_2O)]^{2+}$ WOCs (tpy = 2,2′:6,2″-terpyridine; L = bipyridine or bipyrimidine ligand) showed that the rate determining step is the non-oxidative release of molecular O_2 from a $[Ru(tpy)(L)(O_2)]^{2+}$ complex and re-formation of the initial aqua complex. Addition of excess oxidant or an electrochemical potential results in an extra oxidation step and attack by water on a $[Ru(tpy)(L)(O_2)]^{3+}$ complex to directly form $[Ru(tpy)(L)(OH)]^{2+}$ and increase the rate of O_2 evolution. Thus, the $[Ru(tpy)(L)(O_2)]^{2+}$ complex is a key catalytic intermediate, and its exact structure is a topic of active interest.

Conflicting experimental and theoretical structures have been reported for $[Ru(tpy)(L)(O_2)]^{2+}$.[10–13] Three energetically close-lying structures are possible on two spin surfaces, as shown in Figure 1 for $[\mathbf{Ru}]^{2+}$ (**Ru** = Ru(tpy)(bpy); bpy = 2,2′-bipyridine). On the triplet surface, O_2 binds to the Ru center "end-on", forming a monodentate η^1 complex. On the singlet surface, both an end-on and a bidentate η^2 "side-on" complex are stable species. Crystal structures of related species all have the bidentate η^2 coordination.[14–17]

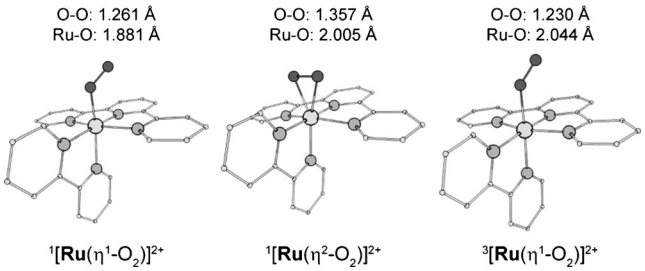

Figure 1. Structures of $^1[\mathbf{Ru}(\eta^1\text{-}O_2)]^{2+}$, $^1[\mathbf{Ru}(\eta^2\text{-}O_2)]^{2+}$, and $^3[\mathbf{Ru}(\eta^1\text{-}O_2)]^{2+}$, calculated at the B3LYP/def2-TZVP(ZORA) level. In $[\mathbf{Ru}]^{2+}$, **Ru** denotes the Ru(tpy)(bpy) fragment.

Concepcion et al.[10] reported the resonance Raman spectrum of a $[Ru(Mebimpy)(bpy)(O_2)]^{2+}$ (Mebimpy = 2,6-bis(1-methylbenzimidazol-2yl)pyridine) solution obtained through ceric ammonium nitrate (CAN) oxidation of the corresponding aqua catalyst. A band at 1015 cm^{-1} was assigned to the O–O stretch based on comparisons with DFT calculations, pointing to the singlet η^2 structure. However, their DFT calculations predicted the triplet η^1 structure as the lowest in energy. Polyansky et al.[18] acquired resonance Raman spectra of a $[Ru(NPM)(pic)_2(O_2)]^{2+}$ (NPM = 4-*tert*-butyl-2,6-di(1′,8′-naphthyrid-2′-yl)pyridine; pic = 4-picoline) solution obtained by bulk electrolysis of the corresponding aqua complex. Spectral changes upon ^{18}O substitution revealed a Ru–O vibration, but no O–O stretch was identified. The authors tentatively assigned the species to the singlet η^2 complex, but the triplet η^1 complex was again energetically favored in their DFT calculations. In a separate theoretical study, Wang et al.[12] found the triplet η^1 complex of $[Ru(tpy)(bpm)(O_2)]^{2+}$ (bpm = 2,2′-bipyrimidine) to be more stable than the singlet structures. They also reported a low 4.4 kcal mol^{-1} barrier and a favorable −15.0 kcal mol^{-1} free energy difference for the H_2O displacement of O_2, both incompatible with the slow kinetics measured for this step.

To clearly identify the binding motif of O_2 with a Ru catalyst and to provide a quantitative comparison with calculations, we present the mass spectroscopic isolation and cryogenic ion IR predissociation spectroscopy of the $[\mathbf{Ru}(O_2)]^{2+}$ complex. Experimental details can be found in the Supporting Information and in Ref. [19]. Electrospray ionization of an aqueous solution of $[\mathbf{Ru}(H_2O)](ClO_4)_2$ (about 1 mM) yielded the $[\mathbf{Ru}(H_2O)]^{2+}$ ion (Figure 2A), which formed the reactive $[\mathbf{Ru}]^{2+}$ species through collisional activation in the high-pressure stages (Figure 2B). The $[\mathbf{Ru}]^{2+}$ ions were exposed to a buffer gas of about 1 % O_2 in He in an 80 K

[*] E. M. Duffy, Dr. B. M. Marsh, J. M. Voss, Prof. E. Garand
Department of Chemistry
University of Wisconsin
1101 University Avenue, Madison, WI 53706 (USA)
E-mail: egarand@chem.wisc.edu
Supporting information and the ORCID identification number(s) for the author(s) of this article can be found under http://dx.doi.org/10.1002/anie.201600350.

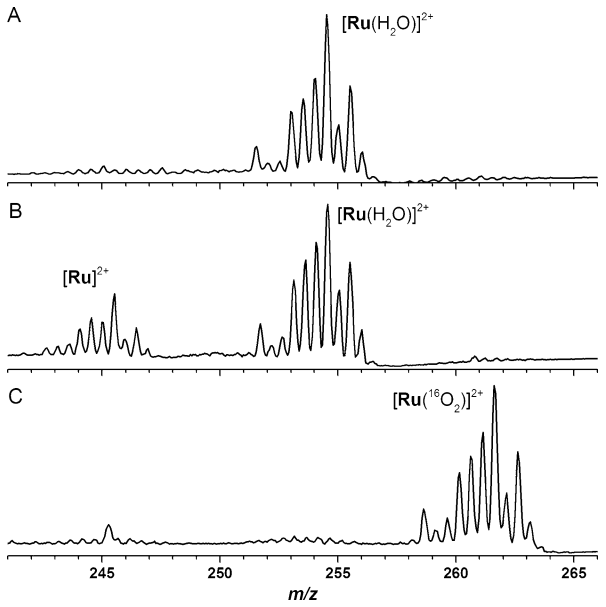

Figure 2. Mass spectra acquired under A) gentle source conditions yielding the $[\mathbf{Ru}(H_2O)]^{2+}$ catalyst, B) collision activation conditions yielding $[\mathbf{Ru}]^{2+}$, and C) the same conditions as in (B) but with additional O_2 present in the 80 K ion trap, resulting in the formation of $[\mathbf{Ru}(O_2)]^{2+}$.

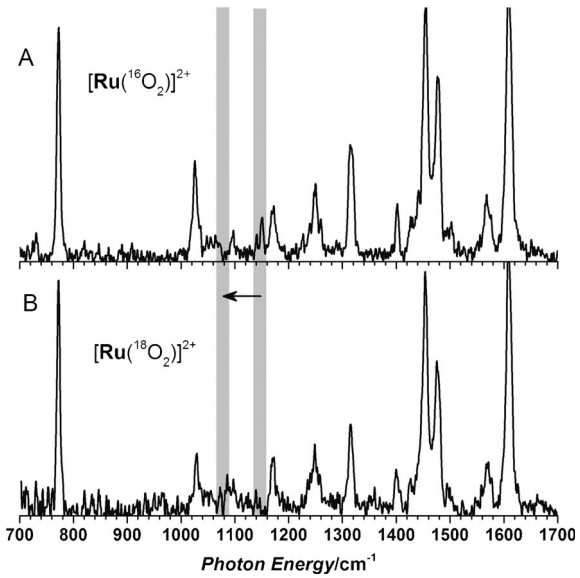

Figure 3. IR predissociation spectra of A) $[\mathbf{Ru}(^{16}O_2)]^{2+}\cdot(D_2)_2$ and B) $[\mathbf{Ru}(^{18}O_2)]^{2+}\cdot(D_2)_2$. Highlighted in gray is a spectral feature that undergoes a red-shift of 65 cm^{-1} upon $^{18}O_2$ substitution.

ion trap to cleanly afford the $[\mathbf{Ru}(O_2)]^{2+}$ complex (Figure 2C). The IR spectrum was acquired directly inside the mass spectrometer using IR predissociation of cold D_2-tagged ions.[20] These tagged $[\mathbf{Ru}\text{-}O_2)]^{2+}\cdot(D_2)_2$ complexes were formed in a second ion trap held at 10 K with a buffer gas of 10 % D_2 in He, and were mass-selected in the time-of-flight spectrometer and irradiated with the output of a tunable IR optical parametric oscillator/optical parametric amplifier (OPO/OPA) laser system. Resonant absorption of a single photon induced the evaporation of the weakly bound D_2 tags, and the resulting photofragment signal was integrated as a function of laser wavelength to produce the IR spectrum. The main advantages of our approach are the clear identification of the complex of interest and the removal of any interference from unreacted complexes, solvent, counterions, and temperature-related effects. Similar methods have been used to characterize other types of reaction complexes.[21,22]

The IR spectra of $[\mathbf{Ru}(^{16}O_2)]^{2+}$ and $[\mathbf{Ru}(^{18}O_2)]^{2+}$ in the 700–1700 cm^{-1} region are presented in Figure 3. All the dominant experimental vibrational features have the same frequency upon $^{18}O_2$ substitution. Close inspection shows that a relatively weak band at 1150 cm^{-1} in the $[\mathbf{Ru}(^{16}O_2)]^{2+}$ spectrum is absent in the $[\mathbf{Ru}(^{18}O_2)]^{2+}$ spectrum, which in turn has a new partially resolved feature at 1085 cm^{-1}. This frequency is within the range of the O–O stretch of many related M–O_2 complexes.[23,24] The band is about 400 cm^{-1} lower than the 1580 cm^{-1} stretch of an isolated O_2 molecule but close to the 1074 cm^{-1} stretch of an isolated superoxide radical anion (O_2^-).[25] Additionally, an isolated O–O stretch at 1150 cm^{-1} would have an isotopic shift of 66 cm^{-1}, in agreement with our experimental measurements. Therefore, we assign the 1150 cm^{-1} and 1085 cm^{-1} features to the ^{16}O–^{16}O and ^{18}O–^{18}O stretches, respectively.

The experimental IR spectrum of $[\mathbf{Ru}(^{16}O_2)]^{2+}$ is compared to the scaled (0.98) calculated harmonic spectra of $^1[\mathbf{Ru}(\eta^2\text{-}O_2)]^{2+}$, $^1[\mathbf{Ru}(\eta^1\text{-}O_2)]^{2+}$, and $^3[\mathbf{Ru}(\eta^1\text{-}O_2)]^{2+}$ in Figure 4. The calculations were performed at the B3LYP/def2-TZVP level using the zeroth-order regular approximation (ZORA)[26] to treat relativistic effects, as implemented in the ORCA[27] program. The Ru–O and O–O bond lengths of the three structures are shown in Figure 1. At this level of theory, the triplet $^3[\mathbf{Ru}(\eta^1\text{-}O_2)]^{2+}$ is the lowest energy structure, similar to previous reports.[10,12,18] The singlet η^1 and η^2 complexes are 5.7 kcal mol^{-1} and 3.4 kcal mol^{-1} higher in energy (including zero-point energy (ZPE) correction), respectively. With the notable exception of the O–O stretch, all three calculated spectra contain similar vibrational features which are in excellent agreement with the experimental spectra. These features correspond to the polypyridyl ligand modes, and the assignments are labeled in Figure 4B. Interestingly, none of the calculated structures yielded an O–O stretch at the experimental 1150 cm^{-1} frequency. The calculated O–O stretch of the singlet η^2 complex is about 80 cm^{-1} too low whereas those of the singlet and triplet η^1 complexes are 100 cm^{-1} and 220 cm^{-1} too high. Additionally, the two η^1 structures have high IR intensities for the O–O stretch, making it the dominant feature in the calculated spectra, in sharp contrast to the experimental spectrum. Conversely, the singlet η^2 structure (Figure 4B), in which the O–O stretch motion is almost totally symmetric with respect to the molecular C_s symmetry plane, has a weak O–O stretch, similar to the experiment. Therefore, we assign the $^1[\mathbf{Ru}(\eta^2\text{-}O_2)]^{2+}$ structure to the experimentally detected species.

The discrepancies between calculation and experiment highlight some shortcomings of the B3LYP treatment of this complex. First, the experimentally detected complex corresponds to an energetically unfavorable structure. It is also

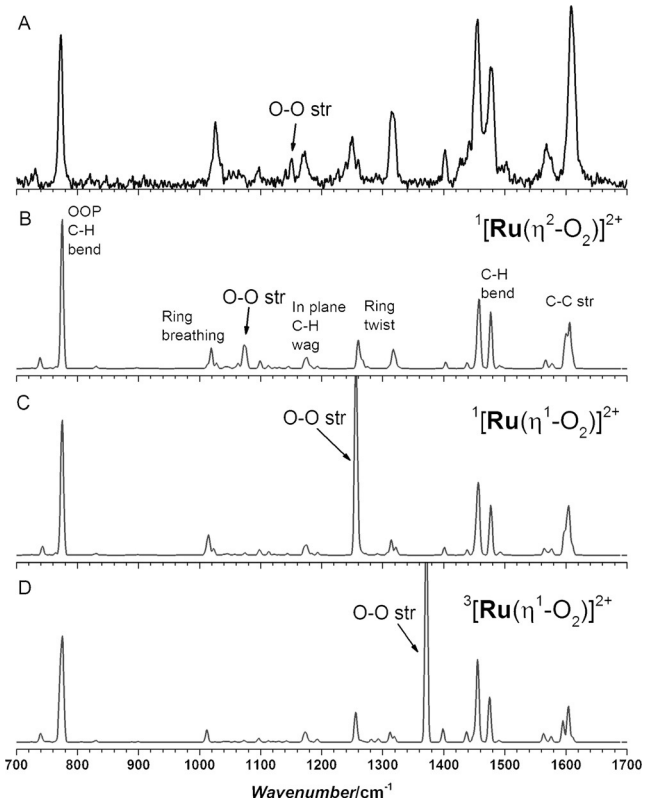

Figure 4. Comparison of A) the experimental IR spectrum of [**Ru**(^{16}O$_2$)]$^{2+}$ with B–D) DFT harmonic spectra, calculated at the B3LYP/def2-TZVP(ZORA) level.

clear that B3LYP is unable to properly capture the Ru–O_2 interaction because the ^{1}[**Ru**(η^2-O_2)]$^{2+}$ structure has an O–O frequency underestimated by about 80 cm^{-1}. Further computational work indicated that the choice of basis set or pseudopotential for Ru effected only minimal changes in relative energies and IR spectra (see the Supporting Information). However, calculations using the B2PLYP double hybrid functional yielded a reversal of the energetic ordering and predicted the ^{1}[**Ru**(η^2-O_2)]$^{2+}$ species as the lowest in energy, with ^{1}[**Ru**(η^1-O_2)]$^{2+}$ and ^{3}[**Ru**(η^1-O_2)]$^{2+}$ 0.7 kcal mol^{-1} and 7.5 kcal mol^{-1} higher in energy (including ZPE corrections calculated from the B3LYP frequencies). Unfortunately, calculations of vibrational frequencies with B2PLYP were not feasible. We note that our B2PLYP results have the same energetic ordering as CCSD calculations of a model ruthenium complex ([Ru(NH$_3$)$_5$(O_2)]$^{2+}$).[13]

The detection of a single [**Ru**(O_2)]$^{2+}$ structure in our experiment at 80 K suggests there is no significant barrier along the [**Ru**]$^{2+}$ + O_2 → [**Ru**(O_2)]$^{2+}$ reaction pathway to trap higher energy species. The reaction likely proceeds via the formation of a η^1 complex on the triplet surface that undergoes rapid intersystem crossing to form the η^1 singlet species, which then yields the η^2 structure. This implies that the rate limiting factor for the reverse reaction would stem mainly from the binding energy of O_2 on the [**Ru**]$^{2+}$ complex. In that regard, B2PLYP predicts an O_2 binding energy of 18.9 kcal mol^{-1} for the ^{1}[**Ru**(η^2-O_2)]$^{2+}$ complex, which is much higher than the B3LYP-calculated 5.3 kcal mol^{-1}. This large difference suggests that a single reference method may not accurately describe these species. The complications likely arise from the open-shell multireference character of the low-lying singlet and triplet states of molecular O_2, which is further complicated by interactions with Ru.[18,28] However, our experimental approach used here to isolate and spectroscopically study the Ru–O_2 interaction provides a clear benchmark for future theoretical work. Furthermore, it should be broadly applicable for characterization of reaction complexes that are otherwise inaccessible by traditional methods.

In conclusion, the IR spectra of the isolated [**Ru**(^{16}O$_2$)]$^{2+}$ and [**Ru**(^{18}O$_2$)]$^{2+}$ complexes are presented. These species, formed and isolated by mass spectrometry, were directly probed in the mass spectrometer by cryogenic ion IR predissociation spectroscopy. The frequency and intensity of the O–O stretch indicate that the O_2 moiety binds to the Ru in a side-on η^2 manner, in agreement with the ^{1}[**Ru**(η^2-O_2)]$^{2+}$ structure. Comparisons with DFT calculations highlight the fact that the B3LYP functional inaccurately describes the Ru–O_2 interaction.

Acknowledgements

The authors thank Prof. John F. Berry for providing the $^{18}O_2$ used in this study. This work was supported by the National Science Foundation under grant number CHE-1454086. The computational resources used in this work are supported by National Science Foundation Grant CHE-0840494.

Keywords: homogeneous catalysis · ion–molecule reactions · IR spectroscopy · laser spectroscopy · reactive intermediates

How to cite: *Angew. Chem. Int. Ed.* **2016**, *55*, 4079–4082
Angew. Chem. **2016**, *128*, 4147–4150

[1] X. Liu, F. Wang, *Coord. Chem. Rev.* **2012**, *256*, 1115.
[2] M. D. Kärkäs, O. Verho, E. V. Johnston, B. Akermark, *Chem. Rev.* **2014**, *114*, 11863.
[3] X. Sala, I. Romero, M. Rodríguez, L. Escriche, A. Llobet, *Angew. Chem. Int. Ed.* **2009**, *48*, 2842; *Angew. Chem.* **2009**, *121*, 2882.
[4] Q. Zeng, F. W. Lewis, L. M. Harwood, F. Hartl, *Coord. Chem. Rev.* **2015**, *304*, 88.
[5] D. J. Wasylenko, R. D. Palmer, C. P. Berlinguette, *Chem. Commun.* **2013**, *49*, 218.
[6] J. J. Concepcion, J. W. Jurss, M. K. Brennaman, P. G. Hoertz, A. O. T. Patrocinio, N. Y. Murakami Iha, J. L. Templeton, T. J. Meyer, *Acc. Chem. Res.* **2009**, *42*, 1954.
[7] J. J. Concepcion, J. W. Jurss, M. R. Norris, Z. Chen, J. L. Templeton, T. J. Meyer, *Inorg. Chem.* **2010**, *49*, 1277.
[8] N. Kaveevivitchai, R. Zong, H.-W. Tseng, R. Chitta, R. P. Thummel, *Inorg. Chem.* **2012**, *51*, 2930.
[9] D. J. Wasylenko, C. Ganesamoorthy, M. A. Henderson, B. D. Koivisto, H. D. Osthoff, C. P. Berlinguette, *J. Am. Chem. Soc.* **2010**, *132*, 16094.
[10] J. J. Concepcion, M.-K. Tsai, J. T. Muckerman, T. J. Meyer, *J. Am. Chem. Soc.* **2010**, *132*, 1545.
[11] Y. Wang, M. S. G. Ahlquist, *Dalton Trans.* **2014**, *43*, 13776.
[12] L.-P. Wang, Q. Wu, T. Van Voorhis, *Inorg. Chem.* **2010**, *49*, 4543.

[13] R. Kang, J. Yao, H. Chen, *J. Chem. Theory Comput.* **2013**, *9*, 1872.
[14] M. E. Navarro Clemente, P. Juárez Saavedra, M. Cervantes Vásquez, M. A. Paz-Sandoval, A. M. Arif, R. D. Ernst, *Organometallics* **2002**, *21*, 592.
[15] G. C. Jia, W. S. Ng, H. S. Chu, W. T. Wong, N. T. Yu, I. D. Williams, *Organometallics* **1999**, *18*, 3597.
[16] E. Lindner, M. Haustein, R. Fawzi, M. Steimann, P. Wegner, *Organometallics* **1994**, *13*, 5021.
[17] J. Y. Shen, E. D. Stevens, S. P. Nolan, *Organometallics* **1998**, *17*, 3875.
[18] D. E. Polyansky, J. T. Muckerman, J. Rochford, R. Zong, R. P. Thummel, E. Fujita, *J. Am. Chem. Soc.* **2011**, *133*, 14649.
[19] B. M. Marsh, J. M. Voss, E. Garand, *J. Chem. Phys.* **2015**, *143*, 204201.
[20] A. B. Wolk, C. M. Leavitt, E. Garand, M. A. Johnson, *Acc. Chem. Res.* **2013**, *47*, 202.
[21] F. S. Menges, S. M. Craig, N. Tötsch, A. Bloomfield, S. Ghosh, H.-J. Krüger, M. A. Johnson, *Angew. Chem. Int. Ed.* **2016**, *55*, 1282; *Angew. Chem.* **2016**, *128*, 1304.
[22] E. Garand, M. Z. Kamrath, P. A. Jordan, A. B. Wolk, C. M. Leavitt, A. B. McCoy, S. J. Miller, M. A. Johnson, *Science* **2012**, *335*, 694.
[23] P. L. Holland, *Dalton Trans.* **2010**, *39*, 5415.
[24] C. J. Cramer, W. B. Tolman, K. H. Theopold, A. L. Rheingold, *Proc. Natl. Acad. Sci. USA* **2003**, *100*, 3635.
[25] K. P. Huber, G. Herzberg, *Constants of Diatomic Molecules* in *NIST Chemistry WebBook*, *NIST Standard Reference Database Number 69* (Eds.: P. J. Linstrom, W. G. Mallard), National Institute of Standards and Technology, Gaithersburg MD, 20899, http://webbook.nist.gov.
[26] D. A. Pantazis, X.-Y. Chen, C. R. Landis, F. Neese, *J. Chem. Theory Comput.* **2008**, *4*, 908.
[27] F. Neese, *WIREs Comput. Mol. Sci.* **2012**, *2*, 73.
[28] M. J. Paterson, O. Christiansen, F. Jensen, P. R. Ogilby, *Photochem. Photobiol.* **2006**, *82*, 1136.

Received: January 12, 2016
Published online: February 17, 2016

